NASA Technical Memorandum 107480

Effect of Flow Misalignment and Multi-Hole Interaction on Boundary-Layer Bleed Hole Flow Coefficient Behavior

David O. Davis
Lewis Research Center
Cleveland, Ohio

Marcus Grimes
United States Military Academy
West Point, New York

Mark Schoe[illegible]berger
Case Western Reserve University
Cleveland, Ohio

Prepared for the
International Mechanical Engineering Congress and Exhibit
sponsored by the American Society of Mechanical Engineers
Atlanta, Georgia, November 17–22, 1996

National Aeronautics and
Space Administration

Effect of Flow Misalignment and Multi-Hole Interaction on Boundary-Layer Bleed Hole Flow Coefficient Behavior

David O. Davis
Internal Fluid Mechanics Division
NASA Lewis Research Center
Cleveland, Ohio

Marcus Grimes
United States Military Academy
West Point, New York

Mark Schoenenberger
Department of Mechanical and Aerospace Engineering
Case Western Reserve University
Cleveland, Ohio

ABSTRACT

The effect of flow misalignment on the flow coefficient behavior of a 20° boundary-layer bleed hole and the effect of the interaction between two 90° bleed holes separated by two hole diameters on flow coefficient behavior has been studied experimentally. Both tests were run at freestream Mach numbers of 0.61, 1.62 and 2.49. The flow misalignment study was conducted over a range of 0 to 30°. The results show that neither flow misalignment nor hole interaction has much effect on the flow coefficient for the subsonic case. For the supersonic cases, flow misalignment causes significant degradation in the performance of the slant hole. For the supersonic normal hole interaction cases, depending on the hole orientation, either an increase or decrease in overall flow coefficient was observed. The largest change in flow coefficient, 6% increase at near choke conditions, occurred when the holes were oriented in line with the flow direction.

NOMENCLATURE

C_f	=	skin friction coefficient
D	=	diameter of bleed hole
H_{inc}	=	incompressible shape factor
L	=	length of bleed hole
$\dot{m}$	=	mass-flow rate
M	=	Mach number
P_{plen}	=	static pressure in bleed plenum
P_t	=	total pressure
Q	=	sonic flow coefficient (Eq. 1)
Re	=	unit Reynolds number
T_t	=	total temperature
y^*	=	subsonic boundary-layer thickness
δ	=	boundary-layer thickness
δ_1	=	displacement thickness
δ_2	=	momentum thickness
θ	=	bleed hole orientation angle (Fig. 3)

Subscripts

e	=	condition at boundary-layer edge
0	=	condition in wind-tunnel plenum

INTRODUCTION

In supersonic aircraft inlets, bleed is often prescribed to control boundary-layer separation and flow distortion stemming from a shock wave and boundary-layer interaction, and also to stabilize the terminal normal shock that resides between the supersonic inlet and the subsonic diffuser. Fig. 1 illustrates a typical boundary-layer bleed region. In this figure, M_e, $P_{t,e}$ and $T_{t,e}$ are the Mach number, total pressure, and total temperature at the boundary-layer edge (freestream), respectively, and P_{plen} is the static pressure in the bleed plenum. The amount of boundary-layer mass that can be removed through a given bleed configuration is usually quantified by the sonic flow coefficient, Q, which is defined as the actual mass flow through a bleed region normalized by the ideal mass

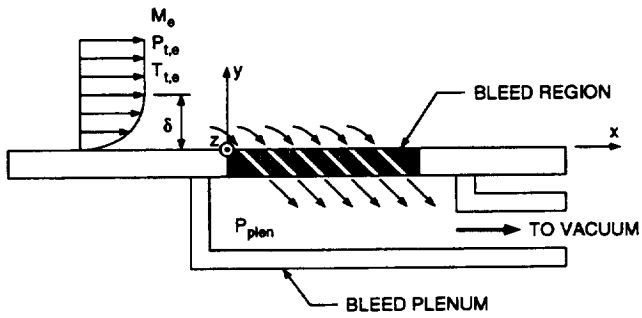

Figure 1 Typical boundary-layer bleed schematic.

flow rate under choked conditions:

$$Q = \frac{\dot{m}}{\dot{m}^*} \tag{1}$$

For air, the ideal choked mass flow in standard liters per minute (slm)* is determined from the following isentropic relation:

$$\dot{m}^*(\text{slm}) = 2.0127 \frac{P_{t,e}(\text{kPa})A(\text{mm}^2)}{\sqrt{T_{t,e}(\text{K})}} \tag{2}$$

where A is the cross-sectional area of the bleed orifice(s). The sonic flow coefficient is usually presented as a function of the bleed plenum pressure normalized by the freestream total pressure ($P_{plen}/P_{t,e}$).

In general, the flow coefficient for a bleed orifice under flow conditions must be determined experimentally. Until recently, the design of bleed systems for supersonic inlets relied largely on the experimental flow coefficient data of McLafferty and Ranard (1958). In their study, flow coefficient distributions were determined for eight round orifice and one rectangular orifice bleed plate configurations. For the round orifice configurations, each bleed plate consisted of two rows of at least six holes per row. The freestream Mach number in the tests ranged between zero and 1.75. Willis *et al.* (1995) extended the flow coefficient database by considering nine additional bleed configurations, which were tested over a Mach number range from 1.27 to 2.46. In addition to sharp-edged round orifices, the configurations tested included the effects of area diffusion and orifice edge treatment as well as single normal and slanted slots. With the exception of the slot configurations, the bleed plates consisted of between three and six rows of orifices. Most recently, Bodner *et al.* (1996) investigated single 90° and 20° round bleed holes at a Mach number of 2.46. In addition to flow coefficient data, surface static pressure in the vicinity of the bleed hole was measured with pressure sensitive paint and cross-plane Pitot pressure and flow angle distributions downstream of the bleed holes were measured with a five-hole probe.

Review of the aforementioned studies reveals two areas of research that warrant further investigation. The first is the effect of flow misalignment on slant hole flow coefficient behavior. In all previous studies, flow coefficient distributions for slant hole configurations were obtained with the approach flow nominally aligned with the bleed hole axis. For this case, the turning of the flow is only in the x–y plane (see Fig. 1). In a real inlet situation, however, flow misalignment may be present and the approach flow would have a velocity component in the z–direction which results in additional flow turning within the hole. When bleed is used to control the glancing shock-wave and side-wall boundary-layer interaction that occurs in a 2–D supersonic inlet, the nominal flow turning due to the shock wave is on the order of 10°. However, near the surface the flow turning can be up to three times the nominal turning.

The second area of interest is the effect of adjacent bleed hole interaction on flow coefficient behavior. Pressure sensitive paint results obtained by Bodner *et al.* (1996) for a single normal hole at a freestream Mach number of 2.46 and near choked bleed

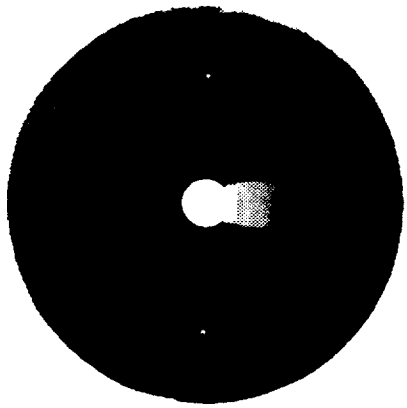

Figure 2 Surface pressure distribution from Bodner et al. (1996), 90° hole, M=2.46, Q=0.034.

conditions are shown in Fig. 2. In this figure, the flow is from left to right and the dark to light grey scale represents increasing surface static pressure. The pressure distribution shows a region of high pressure directly behind the hole and an expansion (low pressure) sweeping back from either side of the hole. A bleed hole placed in proximity to and downstream of an adjacent bleed hole may exhibit a higher or lower flow coefficient depending on the local static pressure level. Changes in the boundary-layer thickness and the generation of secondary flow due to the upstream hole may also influence the flow coefficient of the downstream hole.

EXPERIMENTAL PROGRAM

Two bleed configurations were tested to investigate the effect of slant-hole flow misalignment and normal–hole interaction on flow coefficient behavior. The bleed hole configurations with reference coordinates are shown in Fig. 3. The slant-hole flow misalignment configuration consists of a single 20° hole with a diameter of 6 mm and a length-to-diameter ratio of 2. The normal hole interaction bleed configuration consists of two 90° bleed holes with diameters of 4.572 mm and length-to-diameter ratios of 0.9. The normal holes are separated by a distance of two hole diameters. For both configurations, the bleed holes are machined into a 50.8 mm diameter rotatable plug that is mounted flush into a test section

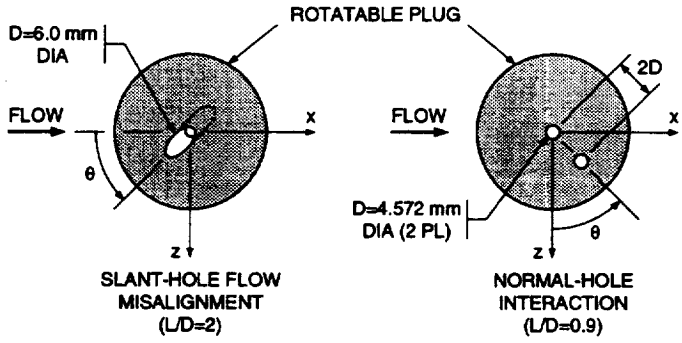

Figure 3 Bleed hole configurations.

* Standard temperature = 293.15° K.

wall of the wind tunnel. The tests were conducted in NASA Lewis' 15×15 cm Supersonic Wind Tunnel, which is an open loop, continuous flow facility with Mach number variation provided by interchangeable nozzle blocks. The tests were conducted at three freestream Mach numbers: M=0.61, 1.62 and 2.49.

The experiment was instrumented to measure the approach boundary-layer profile and the total bleed mass-flow rate. The boundary-layer profiles were measured at a station 36.4 mm upstream of the center of the rotatable bleed plug. The profiles were measured with a round Pitot tube probe having an outer diameter of 0.356 mm. The probe was electrically isolated from the wind-tunnel test section so that wall contact could be established by a continuity check. The mass-flow rate was measured using two techniques. For the M=0.61 case, the mass flow was measured using Omega Model FMA-875–V (200 slm range) and FMA-876–V (500 slm range) mass-flow meters. For the supersonic cases, M=1.62 and 2.49, the mass flow was measured using the ethylene trace-gas technique described by Davis *et al.* (1996). The mass-flow rate through the bleed line was controlled by a motor-driven ball valve. Vacuum for the bleed line was supplied by a Stokes Microvac Model 149–10 mechanical vacuum pump.

The procedure used to obtain the flow coefficient data was to first set the hole orientation angle (θ) and then vary the flow rate through the bleed line via the ball valve. At each data point, the wind-tunnel total conditions, the bleed plenum pressure, and the bleed mass flow were recorded. When a mass flow survey was completed, a new orientation angle was set and the procedure was repeated. Preliminary data for all test cases were taken using the Omega mass-flow meters with a relatively course increment in the orientation angle ($\Delta\theta$=15°). Based on the results of these initial surveys, the data grid was refined and the measurements were repeated using the trace-gas mass flow measurement technique.

RESULTS AND DISCUSSION

Approach Boundary Layer

The approach boundary layer measured at x=-36.4 mm are plotted in Van Driest scaled law-of-the-wall coordinates in Fig. 4. For reduction purposes, the static pressure was assumed to be constant across the boundary layer and equal to the wall static pressure at the measurement station. The wall static pressure was taken to be the average pressure measured with two 0.508 mm diameter taps located at x=-36.4 and z=±20 mm. For the velocity calculations, the temperature distribution across the boundary layer was assumed to follow the adiabatic quadratic Crocco relation using a recovery factor of 0.89 (Laderman, 1978). Pertinent parameters associated with the boundary-layer profiles are given in Table 1. The incompressible shape factor values and the excellent agreement with the theoretical law-of-the-wall profile indicates that the approach boundary layers are fully-turbulent.

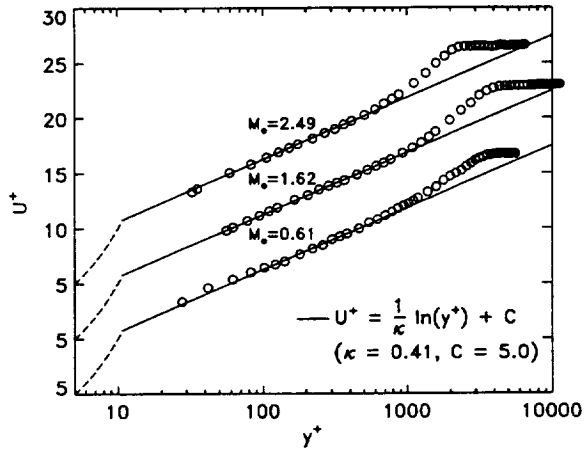

Figure 4 Approach boundary-layer profiles.

Table 1 Approach boundary-layer parameters.

M	0.61	1.62	2.49
$P_{t,0}$ kPa	41.35	114.8	172.3
$T_{t,0}$ K	293	293	293
$Re \times 10^7$ /m	0.460	1.64	1.71
δ mm	22.6	15.0	13.3
δ_1 mm	3.06	2.64	3.44
δ_2 mm	2.10	1.11	0.91
H_{inc}	1.30	1.31	1.32
$C_f \times 10^3$	2.68	1.96	1.68
y^+ mm	22.6	0.83	< 0.18

Slant Hole Flow Misalignment

Flow coefficient distributions for the 20° hole aligned with the flow direction (θ=0°) are shown in Fig. 5 for the three freestream Mach numbers. In this and all subsequent plots, the bleed plenum pressure is normalized by the wind-tunnel plenum pressure, which is assumed to be the same as the boundary-layer edge total pressure, i.e., $P_{t,0}$=$P_{t,e}$. Due to the relatively large pressure drop of the Omega mass-flow meters under vacuum conditions, choked conditions were not obtained for the subsonic test condition. The maximum measured flow coefficient values for the 20° hole

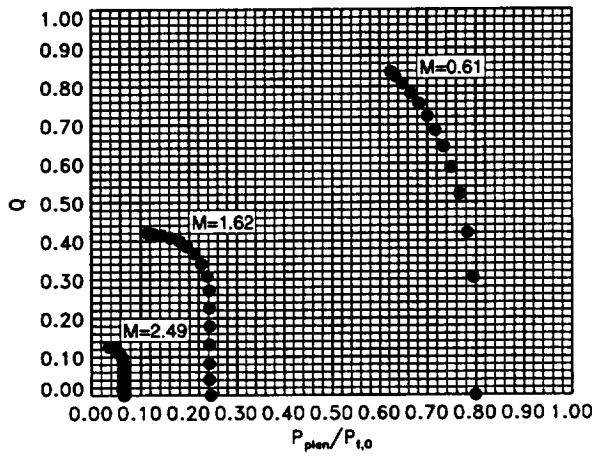

Figure 5 Flow coefficient distributions, 20° hole, θ=0.

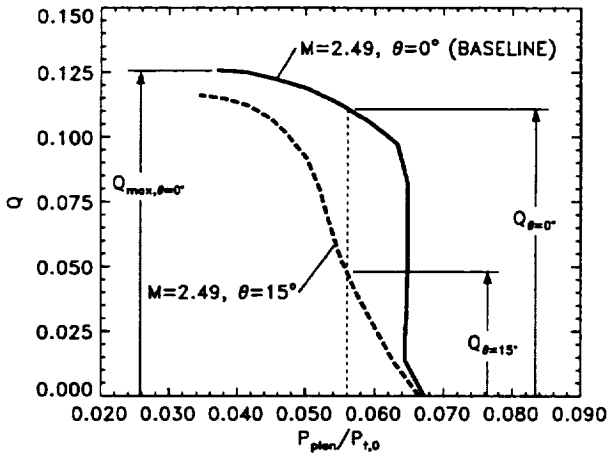

Figure 6 Deviation of flow coefficient curves.

aligned with the flow (θ=0) are given in Table 2. For the supersonic flow cases, the values in the table are very close to choked flow values inasmuch as the slope of the curves in Fig. 5 for the lowest bleed plenum pressure is nearly zero. The flow coefficient curves shown in Fig. 5 represent the baseline to which flow coefficient data under misaligned flow conditions will be compared.

To illustrate the effects of flow misalignment, the flow coefficient data will be plotted as a deviation from the baseline distribution at a given bleed plenum pressure and expressed as a percentage of the maximum measured baseline flow coefficient: $((Q - Q_{\theta=0})/Q_{max,\theta=0}) \times 100$. Fig. 6 illustrates how the deviation is defined for a typical misaligned flow coefficient curve. The maximum measured baseline flow coefficient ($Q_{max,\theta=0}$) values for each Mach number are given in Table 2. The effect of flow misalignment on the 20° hole flow coefficient is illustrated for the three freestream Mach numbers in Fig. 7. Negative deviations (decrease in flow coefficient over the baseline) are plotted as dashed contours. The vertical dotted lines represent orientation angles at which data were obtained.

Table 2 Max. measured Q, 20° hole, θ=0°.

M	0.61	1.62	2.49
Q_{max}	0.839	0.421	0.029

The results for the M=0.61 case are shown in Fig. 7a. These data are the preliminary data obtained with the Omega mass-flow meters. The measurement grid was not refined for this case since the results show that for flow skewness up to θ=30°, there is very little effect on the flow coefficient. The maximum deviation observed is on the order of a half of a percent of the maximum measured baseline flow coefficient.

For the M=1.62 case (Fig. 7b), the deviation from the baseline distribution begins at approximately θ>2.5°. Beyond θ=2.5°, there are two significant changes to the flow coefficient behavior. First, as choked conditions are approached (decreasing $P_{plen}/P_{t,0}$), the maximum flow coefficient value decreases as θ increases. This decrease is on the order of 10% and 20% at skew angles of θ=20° and 30°, respectively. The second change observed is the

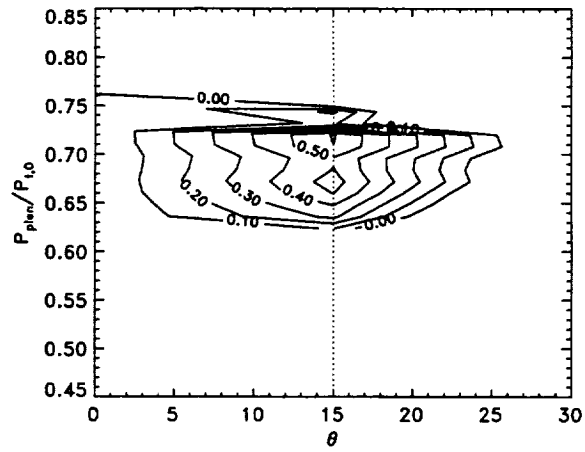

a) M=0.61.

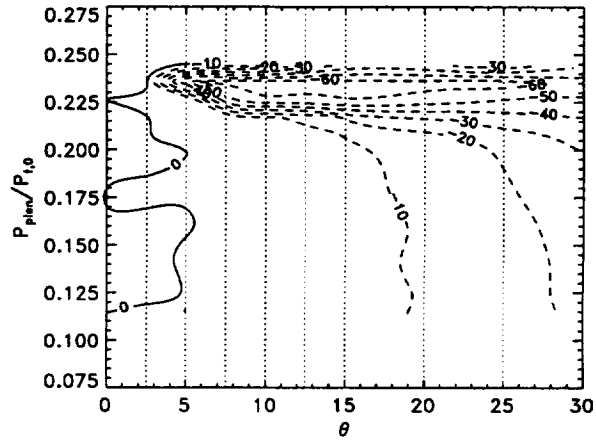

b) M=1.62.

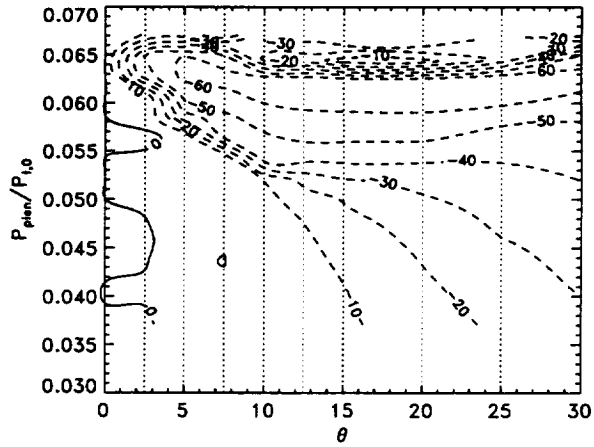

b) M=2.49.

Figure 7 Contours of $((Q - Q_{\theta=0})/Q_{max,\theta=0})$ × 100, single 20° hole.

less rapid rise in flow coefficient as the bleed plenum pressure is initially decreased. With reference to Fig. 5, there is a very rapid rise in the baseline flow coefficient curves as the bleed plenum pressure is initially decreased. Under misaligned flow conditions, however, this initial rise is not so steep and lower bleed plenum pressure is required to attain near-choked bleed flow. Under unchoked conditions, the deviation from the baseline curve can be as high as 60%.

For the M=2.49 case (Fig. 7c), the same general comments as for the M=1.62 case apply, except the deviations are more severe. For instance, deviations from the baseline curve begin at very small flow misalignment angles (θ>2.5°). The decrease in choked flow coefficient as the skew angle increases is also more severe. A 10% decrease in the near-choked flow coefficient occurs at approximately θ=15° as opposed to θ=20° for the M=1.62 case.

The baseline results shown in Fig. 5 support the notion that 20° bleed holes should be operated under choked conditions since the curves exhibit a very unstable nature under unchoked conditions. The bleed system designer must incorporate a sufficient margin of safety into the nominal bleed plenum operating pressure to ensure that a pressure excursion doesn't inadvertently shut off the bleed flow. The results of the present flow misalignment study indicate that if uncertainty in the flow direction exists, then additional bleed area and a lower bleed plenum operating pressure may need to be specified to account for the degradation of bleed hole performance under skewed flow conditions. These adjustments become particularly important at the higher supersonic Mach numbers.

Normal Hole Interaction

Flow coefficient distributions for the 90° holes oriented side-by-side relative to the flow direction (θ=0°) are shown in Fig. 8 for the three freestream Mach numbers. Again, the maximum flow for the subsonic case was limited by the mass-flow meters. The maximum measured flow coefficient values for the 90° holes (θ=0°) are given in Table 3. Unlike the flow coefficient curves for the 20° hole (Fig. 5), the maximum measured flow coefficient for the 90° holes does not correspond to choked conditions since the slope of the curves at the lowest bleed plenum pressure for all cases is non-zero. For the purposes of this part of the study, we

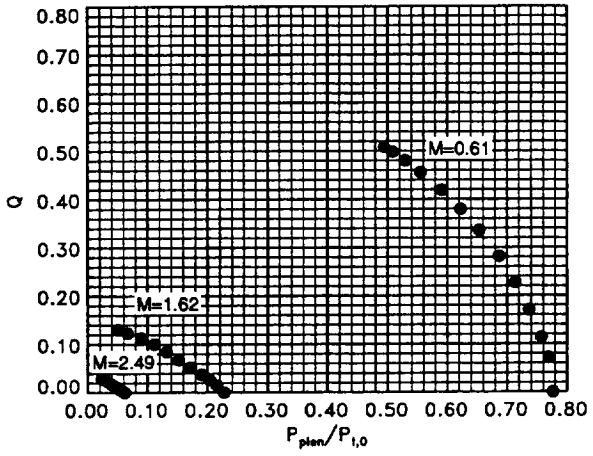

Figure 8 Flow coefficient distributions, 90° holes, θ=0.

Table 3 Max. measured Q, 90° holes, θ=0.

M	0.61	1.62	2.49
Q_{max}	0.509	0.130	0.029

assume that when the 90° bleed holes are oriented side-by-side, there is negligible interaction occurring between them and the flow coefficient curves shown in Fig. 8 represent the baseline to which flow coefficient data under multi-hole interaction conditions will be compared.

The effect of hole interaction on the dual 90° hole flow coefficient is illustrated for the three freestream Mach numbers in Fig. 9. The presentation of the data is the same as described in the previous section. With reference to Fig. 3, the orientation of the bleed holes ranges from side-by-side (θ=0°) to directly in line with the flow direction (θ=90°). As before, the contours in the plots represent the deviation from the baseline (θ=0°) distribution at a given bleed plenum pressure and are expressed as a percentage of the maximum measured baseline flow coefficient (see Table 3). Negative deviations (decrease in flow coefficient over the baseline) are plotted as dashed contours. The vertical dotted lines represent orientation angles at which data were obtained. At this point we should note that the measured data represents the flow coefficient for both holes. In other words, we haven't isolated the effects of the interaction on the individual holes, but it is probable that the downstream hole is more influenced by the interaction than the upstream hole.

Fig. 9a shows the hole interaction results for the M=0.61 case. Although deviations of several percent are observed for low flow rates (high bleed plenum pressure), over most of the operating region the deviation is less than one percent and we conclude that hole interaction has a negligible effect on the flow coefficient for this case.

For the M=1.62 case (Fig. 9b), the deviation from the baseline is nearly always positive (higher flow coefficient) and reaches a maximum of about 4.5%. Unlike the subsonic case, however, the maximum deviation occurs at higher flow rates (lower plenum pressure). The effects of hole interaction for this case begins to appear at about θ=30° and then reach a plateau at about θ=60°. Recall, however, that the measured flow coefficient is for both holes and we can't be certain how much each hole contributes to the increased flow rate. With reference to Table 1, the thickness of the subsonic portion of the boundary layer for the M=1.62 case is significant and upstream influence of the downstream bleed hole is possible. The increase in the overall flow coefficient when one hole is in the wake of the other is probably due to the increased surface pressure behind the upstream hole which is a result of an oblique shock originating in the vicinity of the downstream lip of the upstream hole.

Comparison between the M=2.49 case (Fig. 9c) and the M=1.62 case (Fig. 9b) reveals a qualitative difference in behavior. Whereas the M=1.62 case showed a steady increase in the flow coefficient beginning at θ=30°, the M=2.49 case shows a drop below the baseline for orientation angles between θ=20° and 50° followed by a rise above the baseline until a plateau is reached at approximately θ=75°. The low flow coefficient region reaches a minimum at about 2% below baseline and the high flow coefficient region peaks at about 6% above baseline. With reference

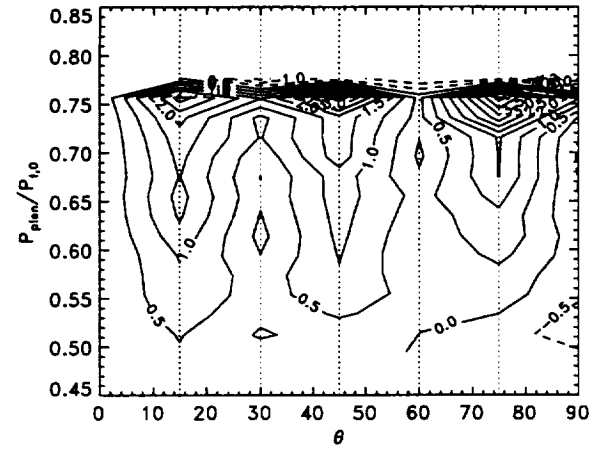

a) M=0.61.

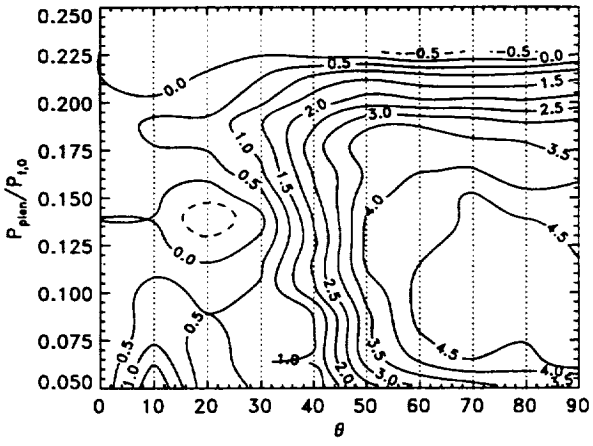

b) M=1.62.

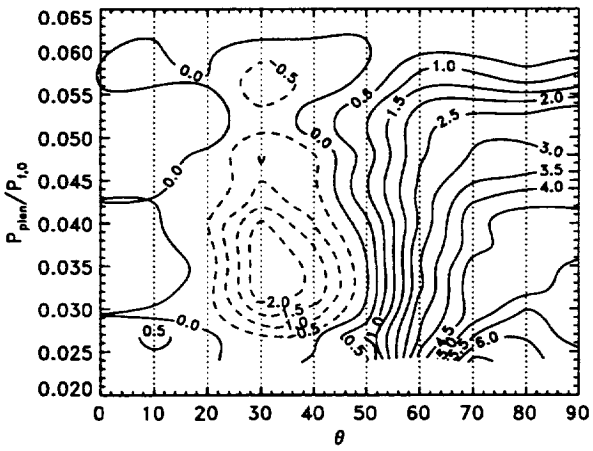

b) M=2.49.

Figure 9 Contours of $((Q - Q_{\theta=0})/Q_{max,\theta=0}) \times 100$, dual 90° holes.

to the pressure sensitive paint results shown in Fig. 2, the flow coefficient behavior of the present study qualitatively correlates well with the surface pressure distribution obtained by Bodner *et al.* (1996).

The results of this multi-hole interaction study suggest that flow coefficient distributions obtained with multi-hole configurations have the potential to exhibit overall higher levels than their equivalent single bleed hole counterpart depending on the layout of the multi-hole configuration.

CONCLUDING REMARKS

An investigation of the effects of slant hole flow misalignment and multi-normal hole interaction on flow coefficient behavior has been conducted. The results of the flow misalignment study show that significant degradation of the bleed hole performance occurs under supersonic flow conditions and should be considered when designing bleed systems. The multi-normal hole study suggests that flow coefficient curves obtained with multi-hole configurations will likely result in higher values than those obtained with the single hole counterpart.

ACKNOWLEDGMENTS

The authors would like to gratefully acknowledge the contribution of Dr. Warren Hingst of NASA Lewis Research Center. They would also like to thank Captain Anne Daugherty of The United States Army for coordinating the Cadet Summer Research Program.

REFERENCES

Bodner, J. P., Greber, I., Davis, D. O.,, and Hingst, W. R., 1996, "Experimental Investigation of the Effect of a Single Bleed Hole on a Turbulent Supersonic Boundary-Layer," AIAA Paper 96-2797.

Davis, D. O., Willis, B. P., Hunter, G. W., Liu, C.-C.,, and Wu, Q., 1996, "Mass Flow Measurement Using a Hydrocarbon Trace-Gas Technique," *Proceedings of the Fluids Engineering Division Summer Meeting*, Vol. 4, FED-Vol. 239, ASME, pp. 465–469.

Laderman, A. J., 1978, "Effect of Wall Temperature on a Supersonic Boundary-Layer," *AIAA Journal*, Vol. 16, pp. 723–729.

McLafferty, G. M., and Ranard, E., 1958, "Pressure Losses and Flow Coefficients of Slanted Perforations Discharging from Within a Simulated Supersonic Inlet," United Aircraft Corporation Report R-0920-1.

Willis, B. P., Davis, D. O.,, and Hingst, W. R., 1995, "Flow Coefficient Behavior for Boundary-Layer Bleed Holes and Slots," AIAA Paper 95-0031.

REPORT DOCUMENTATION PAGE

Form Approved
OMB No. 0704-0188

1. AGENCY USE ONLY (Leave blank)	2. REPORT DATE	3. REPORT TYPE AND DATES COVERED
	June 1997	Technical Memorandum

4. TITLE AND SUBTITLE

Effect of Flow Misalignment and Multi-Hole Interaction on Boundary-Layer Bleed Hole Flow Coefficient Behavior

5. FUNDING NUMBERS

WU-523-36-13

6. AUTHOR(S)

David O. Davis, Marcus Grimes, and Mark Schoenenberger

7. PERFORMING ORGANIZATION NAME(S) AND ADDRESS(ES)

National Aeronautics and Space Administration
Lewis Research Center
Cleveland, Ohio 44135-3191

8. PERFORMING ORGANIZATION REPORT NUMBER

E-10768

9. SPONSORING/MONITORING AGENCY NAME(S) AND ADDRESS(ES)

National Aeronautics and Space Administration
Washington, DC 20546-0001

10. SPONSORING/MONITORING AGENCY REPORT NUMBER

NASA TM-107480

11. SUPPLEMENTARY NOTES

Prepared for the International Mechanical Engineering Congress and Exhibit sponsored by the American Society of Mechanical Engineers, Atlanta, Georgia, November 17-22, 1996. David O. Davis, NASA Lewis Research Center; Marcus Grimes, United States Military Academy, West Point, New York; and Mark Schoenenberger, Case Western Reserve University, Department of Mechanical and Aerospace Engineering, Cleveland, Ohio 44106. Responsible person, David O. Davis, organization code 5850, (216) 433-8116.

12a. DISTRIBUTION/AVAILABILITY STATEMENT

Unclassified - Unlimited
Subject Category 07

This publication is available from the NASA Center for AeroSpace Information, (301) 621-0390.

12b. DISTRIBUTION CODE

13. ABSTRACT ***(Maximum 200 words)***

The effect of flow misalignment on the flow coefficient behavior of a 20° boundary-layer bleed hole and the effect of the interaction between two 90° bleed holes separated by two hole diameters on flow coefficient behavior has been studied experimentally. Both tests were run at freestream Mach numbers of 0.61, 1.62 and 2.49. The flow misalignment study was conducted over a range of 0 to 30°. The results show that neither flow misalignment nor hole interaction has much effect on the flow coefficient for the subsonic case. For the supersonic cases, flow misalignment causes significant degradation in the performance of the slant hole. For the supersonic normal hole interaction cases, depending on the hole orientation, either an increase or decrease in overall flow coefficient was observed. The largest change in flow coefficient, 6% increase at near choke conditions, occurred when the holes were oriented in line with the flow direction.

14. SUBJECT TERMS

Boundary layer control; Orifice flow; Flow coefficients

15. NUMBER OF PAGES

8

16. PRICE CODE

A02

17. SECURITY CLASSIFICATION OF REPORT	18. SECURITY CLASSIFICATION OF THIS PAGE	19. SECURITY CLASSIFICATION OF ABSTRACT	20. LIMITATION OF ABSTRACT
Unclassified	Unclassified	Unclassified	